Neurobiology of Disease

Differential Effects of Tau on the Integrity and Function of Neurons Essential for Learning in *Drosophila*

Stylianos Kosmidis,* Sofia Grammenoudi,* Katerina Papanikolopoulou, and Efthimios M. C. Skoulakis
Institute of Molecular Biology and Genetics, Biomedical Sciences Research Centre "Alexander Fleming," Vari 16672, Greece

Tauopathies are a heterogeneous group of neurodegenerative dementias involving perturbations in the levels, phosphorylation, or mutations of the microtubule-binding protein Tau. The heterogeneous pathology in humans and model organisms suggests differential susceptibility of neuronal types to wild-type (WT) and mutant Tau. WT and mutant human Tau-encoding transgenes expressed pan-neuronally in the *Drosophila* CNS yielded specific and differential toxicity in the embryonic neuroblasts that generate the mushroom body (MB) neurons, suggesting cell type-specific effects of Tau in the CNS. Frontotemporal dementia with parkinsonism-17-linked mutant isoforms were significantly less toxic in MB development. Tau hyperphosphorylation was essential for these MB aberrations, and we identified two novel putative phosphorylation sites, Ser^{238} and Thr^{245}, on WT hTau essential for its toxic effects on MB integrity. Significantly, blocking putative Ser^{238} and Thr^{245} phosphorylation yielded animals with apparently structurally normal but profoundly dysfunctional MBs, because animals accumulating this mutant protein exhibited strongly impaired associative learning.

Interestingly, the mutant protein was hyperphosphorylated at epitopes typically associated with toxicity and neurodegeneration, such as AT8, AT100, and the Par-1 targets Ser^{262} and Ser^{356}, suggesting that these sites in the context of adult intact MBs mediate dysfunction and occupation of these sites may precede the toxicity-associated Ser^{238} and Thr^{245} phosphorylation. The data support the notion that phosphorylation at particular sites rather than hyperphosphorylation per se mediates toxicity or dysfunction in a cell type-specific manner.

Introduction

Tau binds axonal microtubules in CNS and regulates their organization, stability, and function (Buée et al., 2000; Avila et al., 2004). Six Tau isoforms arise in the human CNS by spatiotemporally regulated alternative splicing of a single transcript originating from chromosome 17 (Avila et al., 2004). They contain three or four of the microtubule-binding imperfect repeats (3R or 4R) C-terminally and zero to two N-terminal domains (0N, 1N, and 2N). This diversity may be physiologically significant because 4RTau binds microtubules more efficiently (Buée et al., 2000; DeTure et al., 2000; Geschwind, 2003) and isoforms exhibit differential distribution (Avila et al., 2004; Sergeant et al., 2005).

In humans, elevated wild-type (WT) Tau in the CNS characterizes tauopathies such as Alzheimer's disease (AD), Pick's disease, and progressive supranuclear Palsy among others (DeTure et al., 2000; Lee et al., 2001; Geschwind, 2003; Delacourte, 2005; Goedert, 2005). In contrast, mutations affecting microtubule binding or increasing 4RTau levels (Reed et al., 2001; Goedert, 2005) are causal of frontotemporal dementia with parkinsonism linked to chromosome-17 (FTDP-17). Enhanced phosphorylation on particular sites (Buée et al., 2000; Avila et al., 2004), in patterns characteristic of different tauopathies (Shiarli et al., 2006), is thought causal of decreased microtubule binding, mimicking Tau loss of function. Free Tau could then form toxic cytoplasmic aggregates, thought to result in neuronal dysfunction and neurodegeneration (Geschwind, 2003; Alonso Adel et al., 2004; Trojanowski and Lee, 2005).

Tau-dependent neuronal dysfunction, aggregate formation, and neurodegeneration linked to hyperphosphorylation have been modeled in vertebrate (Lee et al., 2005) and invertebrate (Sang and Jackson, 2005) systems. Focus on the cognitive deficits characteristic of the different tauopathies (Delacourte, 2005) arose because of evidence suggesting that they may precede and be separable from neurodegeneration. In fact, amelioration of cognitive deficits in a mouse model occurred during reduction of WT hTau accumulation, although aggregates continued to form (Santacruz et al., 2005). Consistently, postnatal accumulation of 2N4R hTau in mouse forebrain precipitated learning and memory deficits without aggregates or neurodegeneration (Kimura et al., 2007). Furthermore, learning deficits and impaired hippocampal synaptic transmission without degeneration have been described in mice expressing FTDP-17-linked mutant proteins (Schindowski et al., 2006). This agrees with previous reports of Tau-dependent dysfunction without neurodegeneration in *Drosophila* (Mershin et al., 2004; Mudher et al., 2004; Chee et al., 2005).

However, hTau-dependent neuronal loss has also been reported in mice (Ishihara et al., 2001) and flies (Khurana, 2008).

Received March 27, 2009; revised Oct. 24, 2009; accepted Oct. 29, 2009.

This work was supported by Hellenic General Secretariat for Research and Technology Grants EPAN YB13 (S.K.), PENED 01EΔ207 (S.G.), and ENTER 04EP18 (K.P.). We thank Drs. M. Feany, A. Mudher, J. Botas, G. R. Jackson, J.-M. Dura, and B. Lu for fly strains, T. Tzortzopoulos for generation of transgenic strains, and A. Mudher and the Developmental Studies Hybridoma Bank (University of Iowa, Iowa City, IA) for antibodies.

*S.K. and S.G. contributed equally to this work.

Correspondence should be addressed to Efthimios M. C. Skoulakis, Institute of Molecular Biology and Genetics, Biomedical Sciences Research Centre "Alexander Fleming," 34 Fleming Street, Vari 16672, Greece. E-mail: skoulakis@fleming.gr.

DOI:10.1523/JNEUROSCI.1490-09.2010

 0270-6474/10/300464-14$15.00/0

This may reflect differential Tau phosphorylation and occupation of particular sites rendering the protein dysfunctional, toxic, or both, and it may characterize distinct aspects of the associated pathologies. This is turn is consistent with the apparent differential vulnerability of distinct cell types to WT or mutant Tau levels (Delacourte, 2005) and may reflect the tissue-specific distribution of kinases available to hyperphosphorylate Tau. In *Drosophila*, WT and FTDP-17-linked mutations precipitate specific, often opposing, effects in fly retina toxicity and CNS dysfunction (Grammenoudi et al., 2008). Here we address the question of whether there is specificity in the effects of WT or mutant Tau isoforms on toxicity and dysfunction of the *Drosophila* CNS and whether such differences may be mediated by differential phosphorylation on particular sites.

Materials and Methods

Drosophila *culture and strains. Drosophila* were cultured in sugar–wheat–flour food supplemented with soy flour and $CaCl_2$ (Acevedo et al., 2007) at 25°C unless noted otherwise. All strains were treated with tetracycline for at least two generations before use (Clark et al., 2005) to be free of potential Wolbachia infection. The following fly strains were used: the pan-neural driver *Elav*^{C155}–Gal4 (Robinow and White, 1988; Lin and Goodman, 1994) and *Elav*^{III}–Gal4 on chromosome 3 were obtained from the Bloomington Drosophila Stock Center, and the green fluorescent protein (GFP)-expressing ellipsoid body (EB) driver (Yeh et al., 1995), c232, *UAS–mCD80–GFP* and mushroom body (MB) driver *201Y*–Gal4, *UAS–mCD80–GFP*, and *UAS–mCD80–GFP; OK107*--Gal4 were gifts from J.-M. Dura (University of Montpellier, Montpellier, France). *c772*–Gal4, *UAS–mCD80–GFP*, and *Elav*^{C155}–Gal4; *tubGal80*^{ts} were constructed by standard crosses. The *UAS–htau*^{0N4R}, *UAS–htau*^{R406W}, *UAS–htau*^{V337M} (Wittmann et al., 2001), *UAS–htau*$^{0N4R–E14}$, and *UAS–htau*$^{0N4R–AP}$ transgenic strains that contain human Tau24 were provided by M. Feany (Harvard Medical School, Boston, MA). *UAS–htau*^{2N4R} was a gift from J. Botas (Baylor College of Medicine, Houston, TX), *UAS–htau*^{0N3R} (Mudher et al., 2004) was obtained from A. Mudher (University of Southampton, Southampton, UK), *UAS–htau*^{R406WS2A} (Nishimura et al., 2004) was obtained from B. Lu (Stanford University, Stanford, CA), *UAS–htau*^{2N4RS2A} (Chatterjee et al., 2009) was a gift from G. R. Jackson (University of Texas Medical Branch, Galveston, TX), and *UAS–btau* was from K. Ito (Tokyo University, Tokyo, Japan) (Ito et al., 1997b). *UAS–dtau* transgenics were described previously (Mershin et al., 2004). To generate p*UAS–htau*$^{2N4R–FLAG}$, a fragment coding for the entire 2N4R hTau was amplified from a human tau cDNA hTau40 template using the GoTaq polymerase (Promega) and cloned into the NotI and XbaI sites of the pUAST–FLAG vector. pUAST–FLAG was generated by annealing the oligos 5′-AATTCATGGATTATAAGGACGACGATGACAAGGC-3′ and 5′-GGCCGCCTTGTCATCGTCGTCCTTATAATCCATG-3′ and inserting them between the EcoRI and NotI sites of pUAST (Brand and Perrimon, 1993). The p*UAS–htau*$^{2N4R–STA–FLAG}$ mutant was generated by replacing Ser^{238} and Thr^{245} with Ala using the QuickChange XL site-directed mutagenesis kit (Stratagene) according to the instructions of the manufacturer. The mutagenic oligonucleotides 5′-CCAAGTCGCCGTCAGCTGCCAAGAGCCGCCTGCAGGCAGCCCCCG and 5′-CGGGGGCTGCCTGCAGGCGGCTCTTGGCAGCTGACGGCGACTTGG were annealed onto the p*UAS–htau*$^{2N4R–FLAG}$ plasmid template and contained a silent PvuII restriction site for effective screening of positive clones. The sequence of the mutant was confirmed by dsDNA sequencing (Lark Technologies). Transgenic flies were obtained with standard methods.

Spatiotemporal control of hTau accumulation. Eggs were collected on standard food at 20°C for 2 h. After transferring the parents, the vials were immediately placed at 29°C for 14–15 h to inactivate the Gal80^{ts} protein and expression of the *htau* transgenes throughout embryogenesis. After this transgene induction period, larvae and pupae were allowed to develop until adulthood without additional transgenic protein at 20°C. To induce the transgene specifically during larval stages, egg collection and embryonic development were allowed to proceed at 20°C as described above and then, during hatching and throughout larval development, animals were kept at 29°C and switched back to 20°C during pupariation. To determine the stage of embryonic development critical for MB ablation, flies were kept at 29°C and transferred to a new prewarmed vial every hour. The vials containing eggs were collected for 1 h at 29°C, kept at that temperature for the prescribed time, and then moved to 20°C, and animals were allowed to develop at that temperature until adulthood. The MBs of resultant animals were examined in 2- to 5-d-old adult flies, unless otherwise specified.

Histology. Immunohistochemistry on paraffin sections was performed essentially as described previously (Philip et al., 2001; Mershin et al., 2004). Rabbit anti-LEO (Skoulakis and Davis, 1996) was used at 1:4000 and anti-DRK at 1:1500. Sections from all strains were obtained and processed in parallel in each experiment and were evaluated for MB morphology without knowledge of the genotype. The anti-ELAV (Developmental Studies Hybridoma Bank) was used at 1:200 and anti-DAC at 1:8. For GFP detection in whole-mount preparations, brains of adult flies were processed as described by Leyssen et al. (2005) with minor modifications. Briefly, brains of CO_2 anesthetized flies or third-instar larvae were dissected in PBS (0.04 M NaH_2PO_4 and 1 M NaCl, pH 7.4), fixed for 20 min in 4% paraformaldehyde in PBS at room temperature, washed three times with PBS, and mounted with Dako Mounting medium. Individual 2–3 μm confocal sections were used to construct *z*-stacks. Control brains not expressing GFP were used to set the iris and gain such as to eliminate autofluorescence. Embryos were fixed and stained according to standard protocols (Patel, 1994), and image *z*-stacks were obtained as described above.

Western blotting and antibodies. For Western blotting, *Drosophila* tissue (adult heads, embryos, or larvae) were homogenized in 1× Laemli's buffer (50 mM Tris, pH 6.8, 100 mM DTT, 5% 2-mercaptoethanol, 2% SDS, 10% glycerol, and 0.01% bromophenol blue), and the extracts were heated for 10 min at 95°C, centrifuged at 8000 × *g* for 5 min, and separated in SDS-acrylamide gels. Proteins were transferred to polyvinylidene difluoride membranes and probed with mouse monoclonal anti-Tau 46 (Zymed Laboratories), which targets the C terminus of the protein at 1:3000, and TAU5 (Calbiochem), which targets the proline-rich domain (PRD) at 1:1000, AT100 (Pierce Endogen) at 1:250, the polyclonal antibodies anti-pS262, anti-pS356, and anti-Paired Helical Filament (PHF) (Biosource) were used at 1:2000, and monoclonal antibody AT8 (kindly provided by A. Mudher) was used at 1:200. To normalize for sample loading, the membranes were concurrently probed with an anti-syntaxin primary antibody (8C3; Developmental Studies Hybridoma Bank) at a 1:2000 dilution or anti-tubulin at 1:500. Proteins were visualized with chemiluminescence.

Behavioral analyses. All experiments were performed balanced, so all genotypes involved in an experiment were tested per day and the experimenter was blind to the genotype. Olfactory learning and memory in the negatively reinforced paradigm coupling aversive odors as conditioned stimuli with the electric shock unconditioned stimulus (Tully and Quinn, 1985) was performed essentially as described previously (Philip et al., 2001; Mershin et al., 2004). Olfactory and shock avoidance assays were performed as described previously (Mershin et al., 2004; Acevedo et al., 2007). We refer to the "3 min memory" earliest posttraining performance assessment as learning (Skoulakis and Davis, 1996). Data were analyzed parametrically with the JMP statistical package (SAS Institute) as described previously (Philip et al., 2001; Mershin et al., 2004) and described in the text or figure legends.

Results

Ablation of the mushroom bodies upon pan-neuronal accumulation of human Tau

To investigate whether elevated Tau might affect particular *Drosophila* CNS neurons differentially, we expressed the human 0N4R isoform with the pan-neuronal driver *Elav*. This driver is an appropriate tool to address this question because it is active apparently uniformly in all adult CNS neurons (Robinow and White, 1988, 1991) and transiently in some embryonic neuroblasts and glia (Berger et al., 2007). Neuroanatomical evaluation of the CNS was performed initially with hematoxylin and eosin-

stained paraffin sections of 2- to 5-d-old adult heads. Surprisingly, we noted that, although the overall structure and morphology of the brain appeared unaltered, one major structure, the MBs, seemed severely reduced or entirely absent in the majority of animals (Fig. 1.1–1.3). This is demonstrated in the figure at the level of the dendrites of MB neurons, known as calyces. These structures were prominent in controls (Fig. 1.1, arrow) but not apparent in UAS–$htau^{0N4R}$-expressing animals (Fig. 1.2, arrowhead). Other neuropils such as the protocerebral bridge (Fig. 1.2, arrow) in the posterior of the head and the fan-shaped body (FSB) (Fig. 1.3, arrow) appeared normal. The MBs are bilateral clusters in the dorsal and posterior cortex of the brain, each comprising ~2500 neurons. Their dendrites form the spherical neuropil of the calyx ventral to the cell bodies [Kenyon cells (KCs)], whereas the axons fasciculate into the pedunculus. In the anterior of the brain, the pedunculus bifurcates with processes forming the medial β, β', and γ and the dorsally projecting α and α' vertical lobes (Crittenden et al., 1998; Strausfeld et al., 2003). These neurons are essential for olfactory learning and memory in *Drosophila* and other insects (Menzel, 2001; Heisenberg, 2003; Davis, 2005).

To verify these initial observations, we used the anti-Leo antibody, which is highly preferential for most adult MB neurons (Skoulakis and Davis, 1996; Crittenden et al., 1998; Raabe et al., 2004). Serial sections from heads of $htau^{0N4R}$-expressing animals from independent crosses revealed that all brains displayed defective MBs (Fig. 1). The defects could be categorized into two groups on the basis of severity. Compared with sections from controls (Fig. 1.4, 1.7, 1.10, 1.13, 1.16) processed in parallel, animals with type 1 defects displayed severely reduced, often bilaterally, asymmetrical MBs (Fig. 1.5, 1.8, 1.11, 1.14, and 1.17). Nevertheless, at least one well discernible calyx was present (Fig. 1.5, arrowhead), and, although much reduced, the pedunculus (Fig. 1.8, 1.11, arrowheads) and an apparently intact γ lobe were present (Fig. 1.17, arrowhead). In contrast, animals displaying the much more severe type 2 defects lacked nearly all calycal structures (Fig. 1.6, arrowhead), the pedunculus was nearly absent (Fig. 1.9, 1.12, arrowhead), and the γ lobes were severely malformed and rudimentary (Fig. 1.18, arrowhead). These differences could arise not because the MBs were actually malformed, but because the Leo protein used as an antigenic

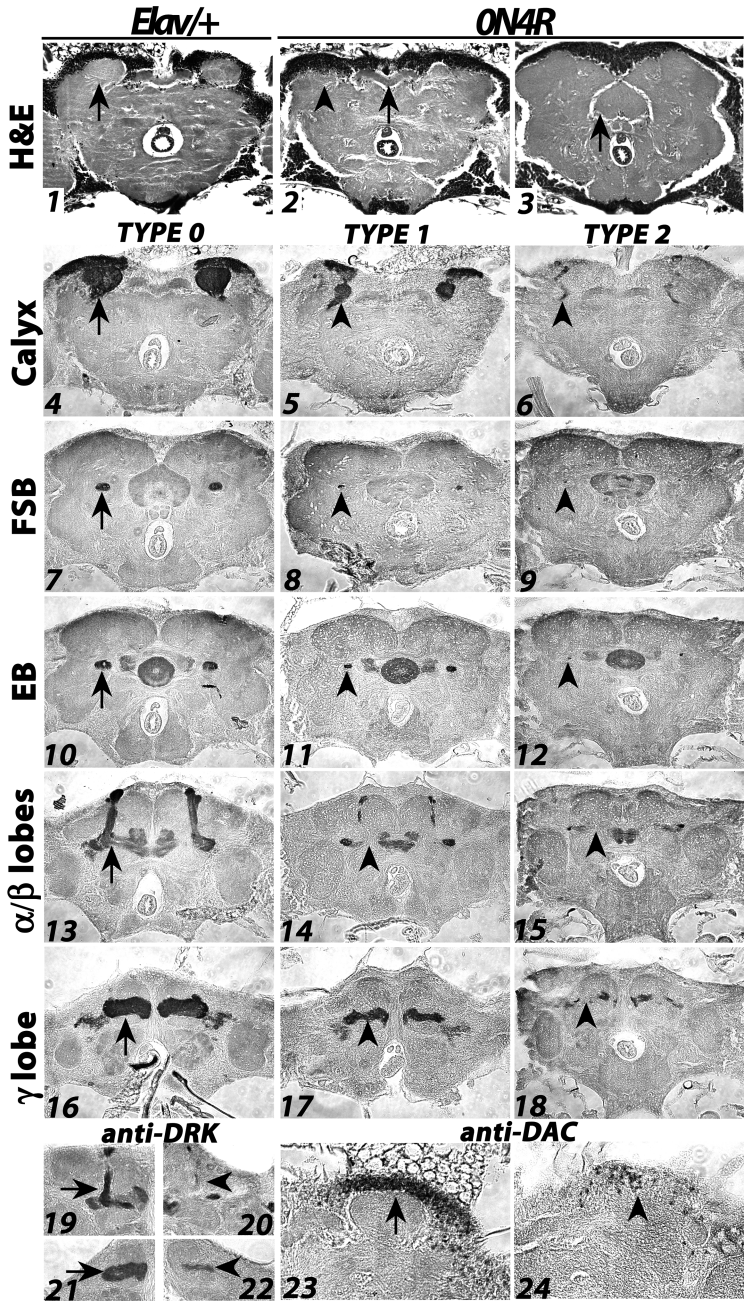

Figure 1. Animals accumulating hTau 0N4R protein harbor aberrant or missing MBs. Panels 1–3 are 4–5 μm Formalin-fixed paraffin-embedded frontal sections of control (1) and hTau-accumulating animals under the pan-neuronal driver *Elav*–Gal4 (2, 3) stained with hematoxylin and eosin (H&E) in the posterior (1, 2) or middle (3) of the head. Arrow in 1 points to the calyces that are not apparent (arrowhead) in hTau-accumulating animals. In contrast, the protocerebral bridge (arrow in 2) and fan-shaped body and noduli (arrow in 3) appear intact in the latter. Panels 4–18 are Carnoy's-fixed paraffin-embedded frontal sections stained with anti-Leonardo. Sections from control brains (4, 7, 10, 13) are arranged from posterior (Calyx) to anterior (γ lobes) as labeled on the left of each row highlighting the most prominent identifiable brain structures. Equivalent sections from hTau-accumulating brains are shown in each row as indicated. The arrows and arrowheads in sections labeled FSB and EB point to the MB pedunculi. Arrows in sections of control brains indicate the normal morphology of MB structures, and arrowheads point to the corresponding aberrations in the sections from experimental brains. Type 0 refers to the normal MBs in control animals (4, 7, 10, 13, 16). Type 1 deficits describe aberrations with still discernable MBs, and type 2 defects describe the near or total loss of MBs. Panels 19–22 are sections at the level of α/β lobes (19, 20) and γ lobes (21, 22) of control (19, 21) and 0N4R hTau-accumulating animals (20, 22) stained with an independent antibody, anti-Drk. Again, arrows point to normal MBs and arrowheads to defects. Panels 23 and 24 show sections at the level of the calyces and Kenyon cells from control and 0N4R hTau-accumulating brain, respectively, stained for the transcription factor Dac. The arrow in 23 indicates the abundant Kenyon cells in control animals that are nearly absent in the experimental brain (arrowhead in 24).

marker could be reduced during Tau accumulation. Thus, we used an additional unrelated antigenic marker, the adaptor protein Drk, which is also preferentially expressed in α, β, and γ lobes of the MBs (Crittenden et al., 1998; Moressis et al., 2009). Again, remnants of few α and β neurons (compare Fig. 1.19 with 1.20) and nearly absent γ lobes were observed (compare Fig. 1.21 with 1.22) in type 2 animals, indicating loss of the structures rather than loss of the antigenic markers. To ascertain this further, we examined the number of corresponding MB cell bodies (KCs), focusing on the subpopulation that express the transcription factor Dac (Martini et al., 2000; Martini and Davis, 2005). Clearly, the cells displaying staining were dramatically reduced in type 2 animals (Fig. 1.24) compared with controls (Fig. 1.23), verifying rarefaction and loss of MB neurons. Therefore, pan-neuronal accumulation of 0N4R hTau disrupts specifically and to near ablation the MB neurons. In contrast, neuropils of the central complex (Strausfeld, 1976), such as the protocerebral bridge (Fig. 1.5, 1.6), FSB (Fig. 1.8, 1.9), EB (Fig. 1.11, 1.12) (supplemental Fig. 1, available at www.jneurosci.org as supplemental material), and antennal lobes (Fig. 1.17, 1.18) (supplemental Fig. 1, available at www.jneurosci.org as supplemental material), remained apparently intact and well organized.

Similar results were obtained with an independent 0N4R WT hTau transgenic line (data not shown) and the also independently generated 2N4R WT hTau and 2N4R–FLAG WT hTau lines (see below), strongly supporting the notion that these structural deficits are not consequences of positional effects of transgene insertion. In congruence with this conclusion, homozygotes for all of the transgene insertions used did not exhibit aberrant CNS neuroanatomy (data not shown). Furthermore, identical MB defects were obtained if the crosses were performed in the reverse orientation (using *Elav* males and scoring the MBs in female progeny) and with an independent *Elav* driver inserted on the third chromosome (Lin and Goodman, 1994) (data not shown), confirming that the effects on MB structure are independent of Gal4 driver, insertion locus, and maternal genotype.

Wild-type and mutant Tau isoforms affect MB structure differentially

Differential effects of WT and mutant isoforms of human Tau on neurodegeneration in *Drosophila* have been reported previously (Wittmann et al., 2001). Our own work revealed differential effects on retinal degeneration and associative learning of various human WT and mutant isotypes (Grammenoudi et al., 2008). We aimed therefore to extend these studies by investigating the effects of Tau isoforms on adult MB integrity. We selected transgenic lines expressing vertebrate Tau at levels differing by 20% or less that of 0N4R, which was assigned as 100% (Fig. 2*A*,*B*). Accumulation of the latter two proteins may be somewhat underestimated because they are larger and may transfer less efficiently during blotting (Fig. 2*B*).

At 25°C, pan-neuronal expression of *dtau*- and *btau*-encoding transgenes did not yield appreciable effects on the MBs (Fig. 2*C*). Of the WT hTau isoforms, 0N3R did not affect the MBs appreciably, in contrast to the 0N4R and 2N4R isoforms that resulted in severe defects specifically of these neurons (Fig. 2*C*) (supplemental Fig. 1, available at www.jneurosci.org as supplemental material). Of the two FTDP-17-linked mutant proteins, V377M hTau yielded milder deficits in approximately half of the brains examined. Deficits consisted mainly of an overall reduction in the size of the MBs, but curiously, in most of the affected animals, the effect appeared mostly unilateral (Fig. 2*C*, Table 1). In contrast, the R406W protein precipitated significantly more severe defects

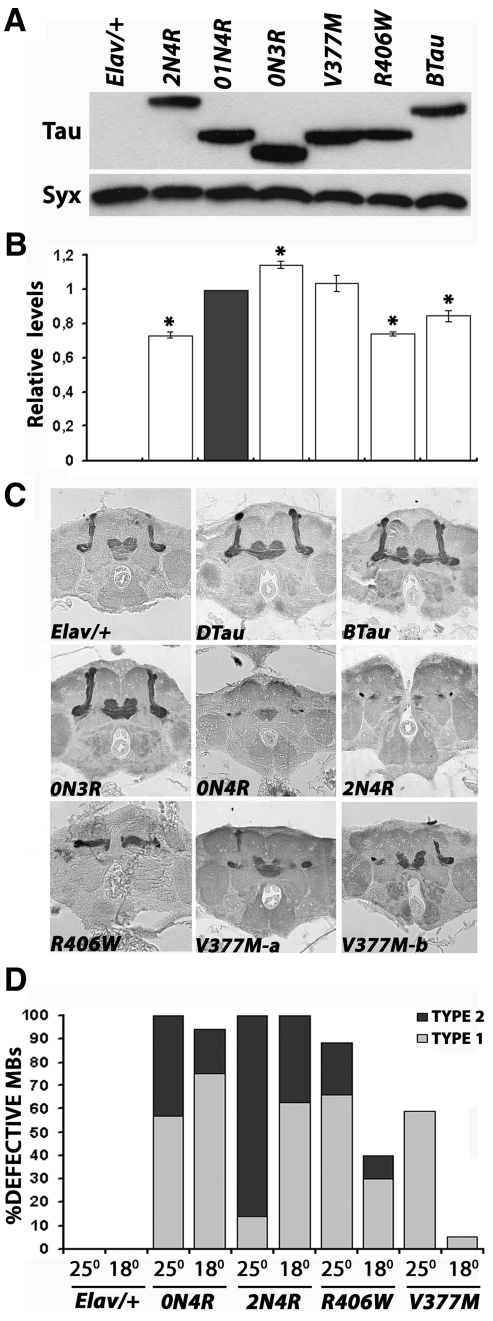

Figure 2. Differential effects on MB integrity of WT and mutant Taus. ***A***, A representative Western blot demonstrating the levels of WT and mutant Tau accumulation under Elav–Gal4 probed with the T46 anti-Tau antibody. The anti-syntaxin antibody (Syx) was used to ascertain equivalent loading of the samples. ***B***, Quantification of the Tau species as indicated in the blot above, relative to the level of 0N4R (black bar) from three independent blots. Dunnett's tests indicated that the differences in accumulation of 0N3R, 2N4R, R406W, and bTau were significantly different (*$p < 0.005$) from the level of 0N4R. ***C***, Carnoy's-fixed paraffin-embedded 5 μm frontal sections at the level of the α/β lobes from control (Elav/+) and animals expressing the indicated WT and mutant Tau isoforms stained with anti-Leonardo demonstrating MB deficits in animals expressing hTau transgenes. The two panels designated ***a*** and ***b*** display sections from two different animals. ***D***, The degree of MB aberrations depends on the type of hTau protein and the levels of its accumulation. The bars display the percentage of animals harboring MB defects, and the shaded portion of the bar indicates the fraction of them displaying the more severe type 2 deficits. At least 15 sections per genotype were evaluated in a single large experiment in which all of the indicated experimental animals were processed in parallel to minimize experimental errors.

Table 1. Quantification of MB aberrations during pan-neuronal Tau accumulation

Tau expressed		MB defects (%)			Total	
Isoform	Mutation	Type 0	Type 1	Type 2	Defective MB (%)	Number of MBs examined
Elav/+		100	0	0	0	16
dTau		100	0	0	0	12
bTau		100	0	0	0	16
0N3R		100	0	0	0	15
0N4R		0	57	43	100	21
2N4R		0	14	86	100	21
0N4R	V377M	41	59[a]	0	59	17
0N4R	R406W	11	66	22	89	18

Collective data from all experimental animals raised at 25°C examined in the survey detailed in Figure 2*C*.

[a]Bilaterally asymmetric MB defects.

generally exhibiting bilateral symmetry (Fig. 2*C*) (see Fig. 5*B*) that clearly remained restricted to the MBs (supplemental Fig. 1, available at www.jneurosci.org as supplemental material). Similar results were obtained with an independent $htau^{R406W}$ transgenic line (data not shown). The collective results of the histological analysis presented above are summarized quantitatively in Table 1. Differences in phenotypic severity between WT and mutant hTau proteins are unlikely a consequence of reduced mutant protein accumulation, because steady-state protein levels appeared equivalent, at least comparing 0N4R with V377M hTau and 2N4R with R406W (Fig. 2*B*). Furthermore, the 2N4R protein precipitated more severe deficits (Fig. 2*C*, Table 1) (also see below), although it appeared less abundant than 0N4R. This contrasts with the more severe effects of the mutant proteins on the integrity of the retina than their WT counterparts (data not shown) as described previously (Wittmann et al., 2001; Khurana et al., 2006).

Furthermore, to demonstrate that the effects on the MBs are dosage dependent, we lowered levels of hTau isoforms that yielded defects by raising the flies at 18°C (Grammenoudi et al., 2006). The results presented quantitatively in Figure 2*D* indicate that reducing the dosage of WT Tau isoforms diminished the proportion of animals exhibiting the more severe type 2 phenotype, but still nearly 100% of the individuals harbored MB defects. Thus, the effects of reducing expression of those WT isoforms that yield phenotypes were primarily quantitative with respect to phenotype severity. In contrast, reducing the levels of the two mutant Tau isoforms had both quantitative and qualitative effects, because it diminished the severity of the defects and the number of animals harboring them in the case of R406W and nearly eliminated the deficits in animals accumulating V377M (Fig. 2*D*). Therefore, the effects of hTau on MB integrity were dose dependent and consistently more severe during accumulation of WT proteins rather than the two FTDP-17 linked mutations. It should be noted that simply increasing the amount of any Tau protein does not suffice to yield MB defects because the highest accumulation level of 0N3R did not affect integrity of these neurons. However, 0N3R accumulation can cause structural and functional deficits in larval motor neurons (Mudher et al., 2004; Chee et al., 2005). This may be a consequence of the reduced number of microtubule binding repeats. In addition, although 2N4R appeared at slightly lower levels than 0N4R (Fig. 2*A*), its effects were consistently more severe. Similar differences in the effectiveness of 2N versus 0N transgenic hTaus in the retina were suggested recently by the work of Chatterjee et al. (2009), indicating that the amino-terminal extension seems to influence hTau toxicity. Collectively then, differences in the consequences of WT and FTDP-17-linked mutant hTau in the *Drosophila* CNS are not likely the result of the relatively small deviations in expression levels or transgene position effects. It appears therefore that phenotypic consequences of WT and mutant Tau accumulation are essentially isoform and mutation specific.

Integrity is compromised by hTau in the embryonic MBs

The effects of Tau accumulation under *Elav* are reminiscent of the previously described hydroxyurea-dependent ablation of MB neurons by mitotic poisoning of their neuroblasts in young first-instar larvae (de Belle and Heisenberg, 1994). In fact, we observed loss of KCs in third-instar larval brains (supplemental Fig. 2, available at www.jneurosci.org as supplemental material) expressing $htau^{0N4R}$ pan-neuronally, whereas neurons in other parts of the CNS appeared unaffected. In addition, parental transmission and early embryonic accumulation of Gal4 under the *Elav* drivers has been reported previously (Tzortzopoulos and Skoulakis, 2007), suggesting that Tau accumulation in the embryo may in fact precede formation of embryonic MB neuroblasts (MBNBs), which also express this driver (Berger et al., 2007).

To determine the developmental period when MB integrity is affected by hTau, we controlled expression of the *tau* transgenes spatiotemporally using the TARGET (Temporal and Regional Gene Expression Targeting) system (McGuire et al., 2003, 2004). Transcription of *tau* transgenes was suppressed by performing crosses at 18°C and was induced by shifting eggs, larvae, pupae, or adults to the permissive temperature of 29–30°C (McGuire et al., 2003). Type 1 and type 2 MB defects were observed in 75% of the adults expressing UAS–tau^{0N4R} under *Elav–Gal4; Tub*–$Gal80^{ts}$ throughout development on to adulthood (Fig. 3*A–C*). This decrease in affected adults from 100% routinely obtained with the *Elav*–Gal4 driver likely reflects incomplete inactivation of the $GAL80^{ts}$ or inadequate hTau at the time window necessary to exert maximal effects attributable to transcriptional delays inherent in the TARGET system. Similarly, 70% of adults expressing $htau^{0N4R}$ exclusively through embryogenesis (see Materials and Methods) harbored MB defects (Fig. 3*A*,*C*), although as expected, Tau was absent from adult brains at the time of histological evaluation (Fig. 3*B*). In contrast, presence of the protein after hatching, from early larvae to adulthood (Fig. 3*B*), yielded mild type 1 defects in <5% of the animals examined (Fig. 3*A*,*C*). Transgene expression exclusively in pupae did not yield detectable defects, and the effects of raising transgene-harboring animals at the restrictive temperature were negligible (Fig. 3*A*,*C*). Therefore, hTau appears to yield defective adult MBs likely because it interferes with their development during embryogenesis.

To establish with more precision the phenocritical period for hTau toxicity on the MBs, embryos collected at the permissive temperature were shifted to restrictive conditions at particular

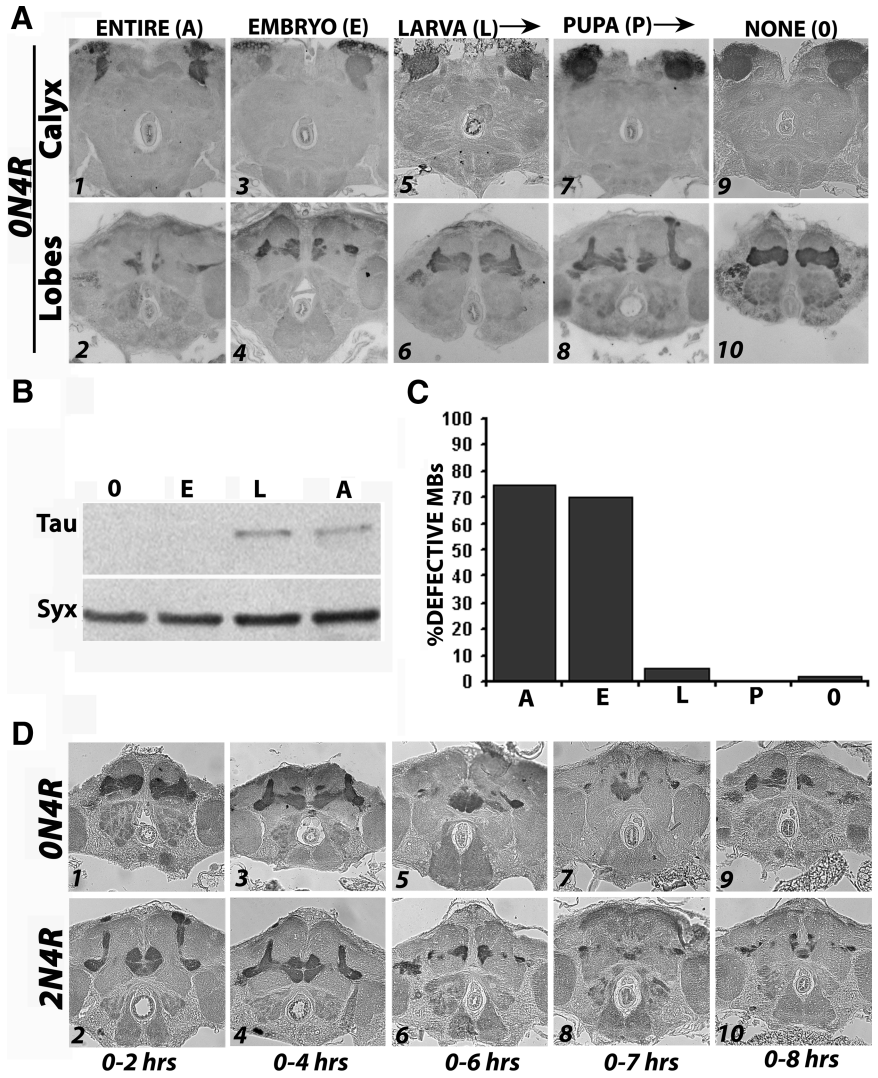

Figure 3. MB defects on pan-neuronal accumulation of hTau arise during embryogenesis. Carnoy's-fixed paraffin-embedded 5 μm frontal sections are shown for all histological evaluations. ***A***, The transcriptional repressor GAL80^{ts} in combination with Elav–Gal4 was used to drive expression of UAS–htau^{0N4R} specifically during the distinct *Drosophila* life stages as detailed in Materials and Methods. The morphology of the MBs in these animals was evaluated with the anti-Leonardo antibody, and sections at the levels indicated on the left are shown. The sections on the top and bottom rows are from different sibling animals. The UAS–htau^{0N4R} was expressed throughout life (A), only during embryogenesis (E), from larval (L) or pupal (P) stages, or none (18°C) onward as indicated. ***B***, Western blot indicating the presence of 0N4R hTau in the heads of animals expressing it from larval stages onward (L) or throughout life (A) and its distinct absence in adult animals that had expressed the transgene only during embryogenesis. The level of syntaxin (Syx) was used as loading control. 0 refers to animals that remained at 18°C throughout the experiment. ***C***, Quantification of aberrant MB phenotypes during limited hTau accumulation in animals raised as detailed in ***A***. $n \geq$ 20 animals examined per condition. ***D***, Determination of the critical period of 0N4R hTau or 2N4R hTau accumulation during embryogenesis, which results in defective or ablated MBs. Severely aberrant MBs were observed in adult flies generated from embryos expressing hTau after 4 h of embryogenesis at 29°C and becomes slightly more severe if accumulation of the protein continues up until 8 h of embryogenesis at that temperature.

times and then allowed to proceed to the end of embryogenesis. Clearly, presence of 0N4R (Fig. 3*D.1*,*D.3*) or 2N4R (Fig. 3*D.2*,*D.4*) hTau in the first 4 h of embryogenesis at 29°C did not affect adult MB structure significantly. In contrast, continued presence of hTau 8 h into embryogenesis yielded adults exhibiting type 1 and type 2 deficits (Fig. 3*D.5–D.10*). Continued Tau accumulation at 29°C up to 14 h after egg laying did not yield more severe deficits (data not shown). Incubation at the permissive temperature for hTau accumulation in the first 4 h of embryogenesis when the zygotic genome is inactive did not result in defective MBs. Therefore, MB toxicity requires zygotic transcription of the *htau* transgenes. However, hTau accumulation immediately after (4–6 h) (Fig. 3*D.5*,*D.6*) yielded maximal MB aberrations. This suggests that hTau may affect the formation, survival, or proliferation of MB neuroblasts born during that period and when the transgenes are expressed under *Elav*–Gal4 (Tzortzopoulos and Skoulakis, 2007).

To investigate how hTau affects the embryonic MBs, we used the anti-Dac antibody to track cells of the MB neuroectoderm (MBne), known to give rise to MBNBs and eventually the embryonic MB (Younossi-Hartenstein et al., 1996; Noveen et al., 2000). Although Dac is not expressed only in the MB lineage, it is an excellent marker for this purpose because its stereotypical expression pattern is well mapped (Noveen et al., 2000), and it is clearly expressed in the neuroblasts that delaminate from the procephalic ectoderm (MBne). Furthermore, because it marks additional lineages of the embryonic head ectoderm, the relative effects of hTau on different cell types can be determined. Compared with control embryos, cells at the stereotypical MBne location in the head of stage 9–12 $hTau^{0N4R}$-expressing embryos were not apparent by Dac staining. However, adjacent cells of the unrelated paraMB neuroectoderm (paraMBne) remained Dac positive (Fig. 4*A.1–A.5*). By stage 14 (Fig. 4*A.6*), the location in the posterior CNS expected to be occupied by Dac-positive embryonic KCs was devoid of signal, whereas other Dac-positive groups of cells such as those of the optic lobe primordium appeared unaffected. This was also readily apparent by stage 16, when few, if any, Dac-positive cells appeared in the dorsal posterior brain of $hTau^{0N4R}$-expressing embryos in which the KCs normally reside (Fig. 4*A.7–A.9*). In contrast, other CNS cell types did not show obvious defects, at least as revealed by the neuroanatomy and Dac staining of transgene-expressing embryos (Fig. 4*A*), larvae (supplemental Fig. 2, available at www.jneurosci.org as supplemental material), and adults (Fig. 1) .

The data are consistent with previous reports using time-restricted expression of the activated Notch intracellular fragment during stages 9–10. This treatment abolished neuroblast delamination resulting in significant reduction or loss of Dac-positive MB neurons (Struhl et al., 1993; Hartenstein et al., 1994; Noveen et al., 2000). These specific effects, along with our data, likely reflect the unique developmental program of MB intrinsic neurons. All MB neurons per brain hemisphere arise from four MBNBs and their progeny ganglion mother cells (GMCs) (Ito et al., 1997a). MB neuroblasts are exceptional because, unlike the rest of the CNS neuroblasts, they maintain their proliferative activity throughout development (Ito and Hotta,

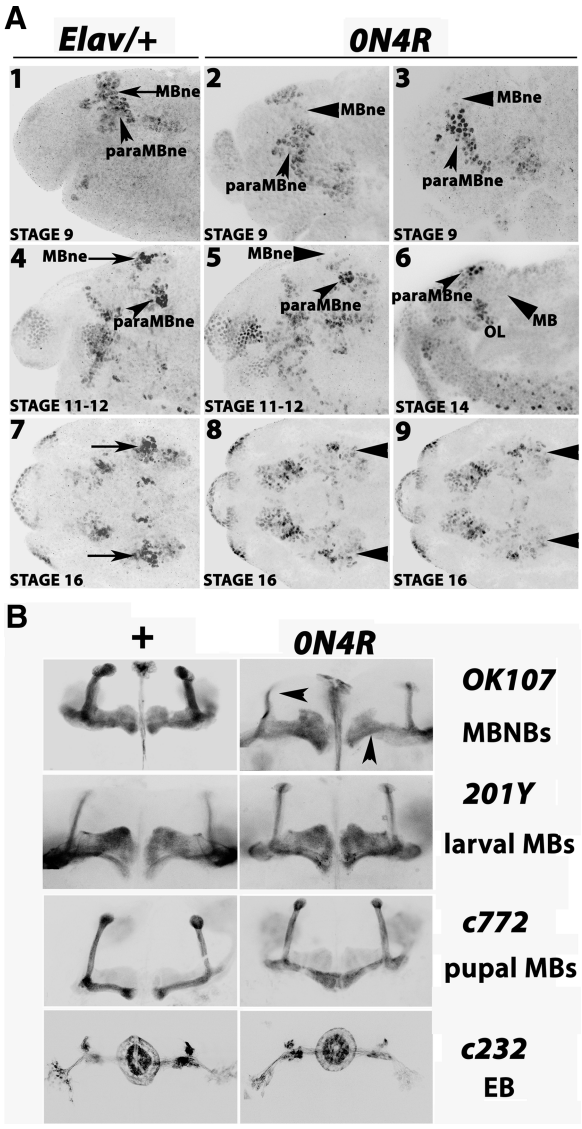

Figure 4. Loss of embryonic MB neuroblasts during hTau accumulation. ***A***, Embryos accumulating 0N4R hTau under Elav–Gal4 were stained with the anti-Dac to visualize the MBne and their lineage during CNS development. Equivalent stacks of confocal images are shown after conversion to grayscale and inversion for clarity. Anterior is to the left. Expected location and identity of Dac-positive cells are as described by Noveen et al. (2000). Arrows point to Dac-positive cells (1, 4, 7), and arrowheads (2, 3, 5, 6, 8, 9) indicate their absence or severe reduction. Absence of MBne cells and their progeny was apparent in hTau-accumulating stage 9 embryos in contrast to controls (Elav/+). Note that the adjacent cluster of Dac-accumulating cells paraMBne appeared essentially unaffected. Similar differences between control and experimental embryos were observed at stages 11–12 and 14, in which there is marked absence of signal where the MBs (MB) were expected. However, cells of the optic lobe (OL) primordium retain Dac staining and are found in their expected location. By stage 16, the MBs are apparent as Dac-positive clusters in the posterior of the CNS of control embryos (arrows), whereas they are severely reduced or nearly absent (arrowheads) in embryos accumulating 0N4R hTau. ***B***, Adult MB morphology examined in dissected brains coexpressing 0N4R hTau along with mCD80–GFP or mCD80–GFP alone (+) under the indicated Gal4 drivers. The earliest known expression in the MBs under the relevant drivers is indicated. Stacked confocal images of GFP fluorescence were converted to grayscale and inverted to reveal detail.

1992). This predicts that early interference with the survival or developmental program of MBNBs would grossly alter MB intrinsic neuron number, resulting in adults with vestigial and aberrant MBs. In agreement, expression of *hTau* transgenes throughout development does not yield significantly enhanced MB aberrations compared with its presence strictly during embryogenesis, indicating that MBNBs, GMCs, or early embryonic MB neurons are specifically affected. The results indicate that hTau may promote MBNB quiescence, suppress their survival, or alter the fate of MBNBs and perhaps GMCs.

Because the area typically occupied by the MBs in the embryo or the adult appears devoid of cells exhibiting the characteristic "collapsed" morphology especially in the presumptive calycal area (Fig. 1.2, 1.6, 1.24), it is unlikely that hTau alters the fate of MBNBs and early neurons. In agreement, anti-Repo staining did not reveal supernumerary glia in that location (data not shown). Loss of Dac-positive cells as early as from the MBne suggests that hTau accumulation may in fact result in their death. However, coexpression of the baculovirus anti-apoptotic protein p35 (Zhou et al., 1997) with 0N4R or 2N4R did not alter perceptively the MB aberration phenotype (data not shown). This indicates that apoptotic cell death of MBNBs or MB neurons is an unlikely explanation of the phenotype. Therefore, it appears that the hTau-dependent MB defects may result from suppression of MB progenitor cell proliferation. In agreement with the embryonic origin of the phenotype, 0N4R or other hTau isoforms (data not shown) expressed in MBs of late pupae and adults under *c772* were not toxic (Fig. 4*B*). Similarly, the MBs appeared unaffected under *201Y*, a Gal4 driver expressed mostly during larval stages (Tettamanti et al., 1997). In contrast, when $htau^{0N4R}$ was expressed in MBNBs and their progeny under the embryonic MBNB-expressing *OK107* (Zhu et al., 2006) (supplemental Fig. 3, available at www.jneurosci.org as supplemental material), animals with obvious deficits were obtained (Fig. 4*B*). However, the MBs were not affected as grossly as under *Elav*, perhaps because of comparatively lower protein accumulation or delayed accumulation in MBNBs under *OK107*. As expected, 0N4R hTau limited to the ellipsoid body under driver *c232* was not toxic for these neurons (Fig. 4*B.7*,*B.8*). Similar results were obtained with the apparently more pathogenic (see below) (supplemental Fig. 3, available at www.jneurosci.org as supplemental material), pseudo-hyperphosphorylated E14 mutant of the 0N4R protein (Khurana et al., 2006).

hTau hyperphosphorylation disrupts MB development

Previous reports suggest that, as in human patients (Buée et al., 2000; Augustinack et al., 2002), hTau hyperphosphorylation is necessary for its pathogenic effects in *Drosophila* (Khurana et al., 2006; Steinhilb et al., 2007a,b). To assess whether hTau hyperphosphorylation is required for MBs toxicity, we took advantage of two highly modified 0N4R hTau transgenes. In the $htau^{0N4R-E14}$ transgene, 14 serines and threonines, most typically phosphorylated in cases of human pathology have been mutated to glutamate mimicking permanent phosphorylation at these sites (Khurana et al., 2006; Steinhilb et al., 2007b). In contrast, the same serines and threonines have been mutated to alanines in $htau^{0N4R-AP}$ (Fulga et al., 2007), rendering these sites phosphorylation incompetent. Both mutant *hTau* transgenes were expressed under *Elav* at 25°C or 29°C, and MB morphology was assessed in 1- to 3-d-old adults. The MBs were normal in control animals under both conditions (Fig. 5, *A.1*,*A.1′* vs *A.2*,*A.2′*) but, as expected, 0N4R yielded modest and severe deficits at 25°C and 29°C, respectively. $0N4R^{E14}$ hTau at 25°C resulted in severe type 2 phenotypes similar to those exhibited by elevated 0N4R at 29°C (Fig. 5*A.5*,*A.5′*) and more extreme phenotypes displaying very few Leo-positive cells where the MBs would be expected (Fig. 5*A.6*,*A.6′*). Similar results were obtained if $0N4R^{E14}$ hTau was restricted specifically to early embryos using the TARGET system. In contrast, the phosphorylation-suppressed $0N4R^{AP}$ pro-

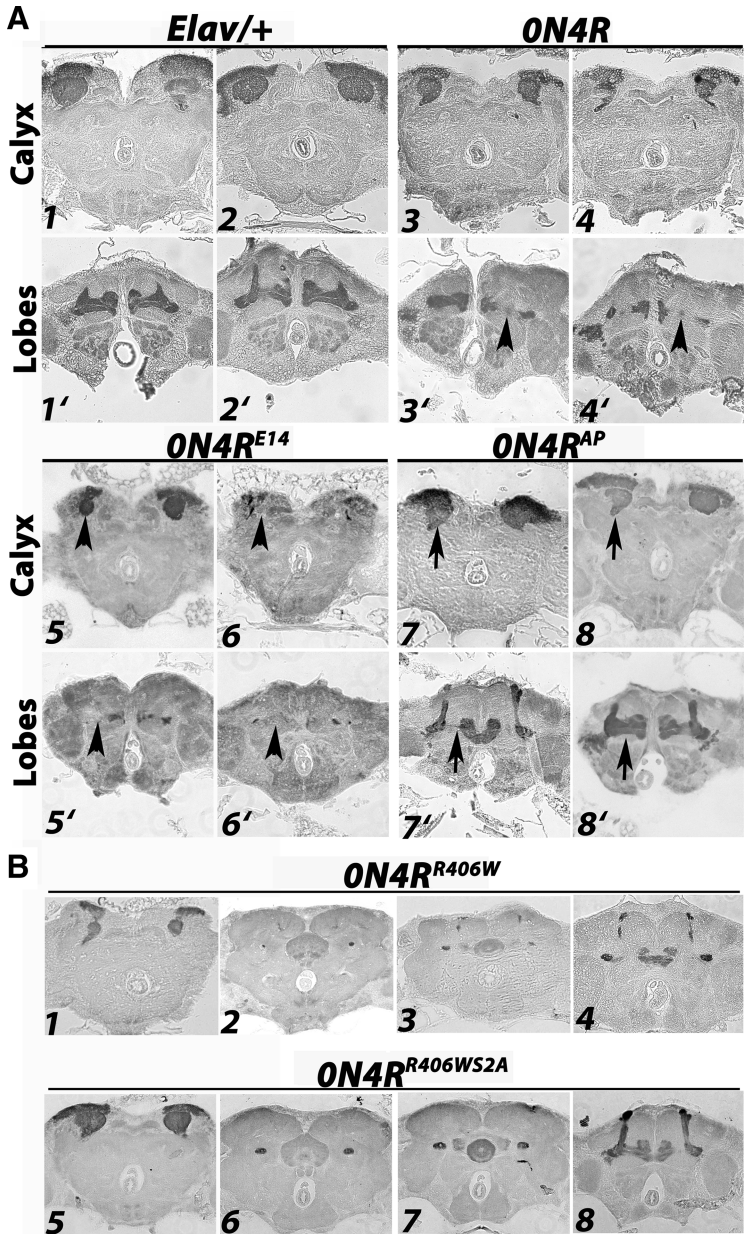

Figure 5. hTau phosphorylation is essential for MB ablation. Carnoy's-fixed paraffin-embedded 5 μm frontal sections are shown for all histological evaluations. ***A***, The left columns display sections at the indicated levels from animals raised at 25°C, and the right column display sections from animals raised at 29°C. MBs remained intact in control flies raised at either temperature (1, 1′) versus (2, 2′). In contrast, the phenotype of 0N4R hTau was more severe at 29°C (4, 4′), consistent with higher accumulation of the protein than in flies raised at 25°C (3, 3′). Flies accumulating the phosphomimic mutant 0N4R^{E14} hTau displayed severe MB perturbation at 25°C (5, 5′), becoming even more severe at 29°C (6, 6′). In contrast, accumulation of the underphosphorylated 0N4R^{AP} hTau variant did not yield MB perturbations at 25°C (7, 7′) or 29°C (8, 8′). ***B***, Type 1 MB alterations in a typical 0N4R^{R406W} hTau-accumulating animal and complete reversal of the phenotype in animals accumulating the 0N4R^{R406WS2A} hTau variant. Sections at the level of the calyces (1, 5), the fan-shaped body (2, 6), the ellipsoid body (3, 7), and the lobes (4, 8) are shown.

tein did not precipitate any appreciable deficits at either temperature (Fig. 5*A.7*,*A.7*′,*A.8*,*A.8*′), although transgene expression was generally higher than that of *htau*$^{0N4R–E14}$. The extreme phenotypes observed with 0N4R^{E14} compared with those yielded by 0N4R suggest that the WT hTau protein may be less extensively phosphorylated, at least on these 14 sites, during the phenocritical period, or the Glu substitutions render the 0N4R^{E14} protein more toxic. These results indicate that hyperphosphorylation of hTau is essential for toxicity on developing MBs. However, even in the more extreme cases of 0N4R^{E14} accumulation, few MB neurons remained. This indicates that, as suggested above for WT hTau isoforms, MBNB proliferation rather than survival seems to be suppressed by hTau.

Toxicity of hTau in the *Drosophila* retina is affected by Par-1 because it phosphorylates Ser^{262} and Ser^{356}, whose occupation facilitates (primes) phosphorylation at additional sites (Nishimura et al., 2004). This is particularly evident on Thr^{212} and Ser^{214} (AT100 epitope), whose hyperphosphorylation is typically associated with human neurodegenerative conditions (Buée et al., 2000; Lee et al., 2001). Therefore, we investigated the contribution of these sites on MB toxicity by using transgenes in which Ser^{262} and Ser^{356} were mutated to alanines (R406WS2A). Because transgenes bearing these mutations were available in the 0N4R^{R406W} hTau mutant background (Nishimura et al., 2004), we used the latter transgenics as controls. As expected, R406W accumulation precipitated deficits at 29°C (Fig. 5*B.1–B.4*). In contrast, accumulation of R406WS2A was not toxic on MB development, even at 29°C, in which transgene expression was elevated as expected (Fig. 5*B.5–B.8*). Therefore, phosphorylation of Ser^{262} and Ser^{356} by Par-1 appears requisite for MB toxicity as is in the retina (Nishimura et al., 2004; Chatterjee et al., 2009). Furthermore, we examined the MBs in animals homozygous for the *Elav* driver and the UAS–*htau*^{R406WS2A} insertion, which contain R406WS2A levels far exceeding that in *Elav*/+; UAS–*htau*^{0N4R}/+ (supplemental Fig. 4*A*, available at www.jneurosci.org as supplemental material). Even these *Elav*; UAS–*htau*^{R406WS2A} animals retained normal MB morphology (supplemental Fig. 4*B*, available at www.jneurosci.org as supplemental material). Therefore, MB defects are not precipitated simply from a large hTau excess, arguing against nonspecific toxicity as causal of the phenotype. Rather, it seems that Tau toxicity on MBNBs depends strongly on its phosphorylation potentially on particular residues.

In addition, at the completion of this study, we obtained transgenic flies carrying the S262A and S356A mutations on 2N4R WT hTau (Chatterjee et al., 2009). In agreement with the results with 0N4R R406WS2A, pan-neuronal accumulation of 2N4RS2A at equal levels with the 2N4R controls (supplemental Fig. 4*C*, available at www.jneurosci.org as supplemental material) did not affect MB morphology (supplemental Fig. 4*D*, available at www.jneurosci.org as supplemental material). Therefore, phosphorylation of these two Par-1-targeted serines seems critical for WT and mutant hTau toxicity in the MBNBs.

Novel mutations on 2N4R hTau suppress toxicity but yield dysfunctional MBs

In contrast to WT hTau proteins, approximately equivalent expression of the *btau* transgene under *Elav* (Mershin et al., 2004; Grammenoudi et al., 2006) did not precipitate obvious MB defects (Fig. 2) (Mershin et al., 2004). However, targeting bTau specifically to the adult MBs yielded learning and memory deficits, consistent with functional disruption of these neurons (Mershin et al., 2004). Sequence alignment of these two Tau proteins revealed high amino acid conservation, with differences primarily concentrated at the N termini and the N-terminal part of the PRD. The remaining sequence appeared invariant except that, in bTau, alanines replaced Ser^{238} and Thr^{245}, whereas a Gly replaced Val^{248} in the C-terminal part of the PRD and microtubule binding domain 1 of hTau, respectively (supplemental Fig. 5*A*, available at www.jneurosci.org as supplemental material). Because phosphorylation is essential for Tau-dependent MB toxicity, we concentrated initially on the potentially phosphorylatable residues Ser^{238} and Thr^{245}. Both residues are predicted targets of the atypical PKCδ (http://networkin.info/search.php), but Thr^{245} has also been suggested as a target of Rho kinase in PC12 cells (Amano et al., 2003). Ser^{238} and Thr^{245} have actually been reported phosphorylated in samples from human AD patients by mass spectrometry (Sergeant et al., 2008), suggesting that they may play a role in neuronal dysfunction or degeneration. Nevertheless, these are novel sites because they have not been studied functionally and were not altered in the $0N4R^{E14}$ (Khurana et al., 2006), $0N4R^{AP}$ (Steinhilb et al., 2007a), or $2N4R^{S11A}$ (Chatterjee et al., 2009) transgenes. Therefore, we changed these two amino acids in a FLAG-tagged WT 2N4R hTau to nonphosphorylatable alanines yielding the 2N4R-STA FLAG-tagged protein. Histological evaluation of the MBs in adults expressing $htau^{2N4R–STA}$ throughout development did not reveal obvious morphological defects, in contrast to animals harboring the control 2N4R–FLAG-tagged protein (Fig. 6*A*), although both proteins accumulated equivalently (Fig. 6*B*). This surprising result demonstrates that blocking putative phosphorylation at two novel sites, previously not associated with Tau-dependent pathogenesis, was sufficient to fully suppress 2N4R hTau toxicity on the MBs. Therefore, it appears that Ser^{238} and Thr^{245} and potentially their phosphorylation are important for the toxic effects of hTau on the MBNBs. These results are also consistent with the lack of toxicity during bTau accumulation, because these residues are alanines in the bovine protein.

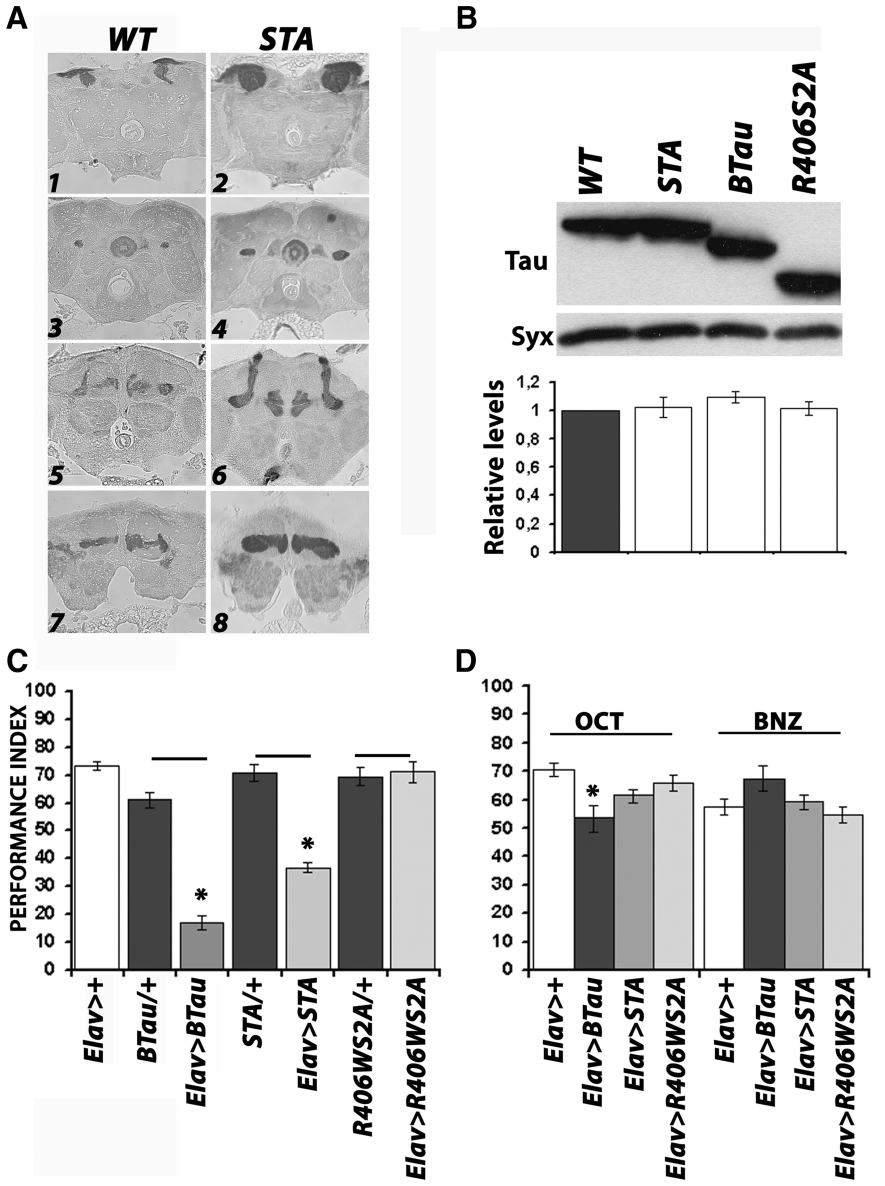

Figure 6. Behavioral deficits in animals accumulating Tau variants that do not perturb MB structure. ***A***, Carnoy's-fixed paraffin-embedded 5 μm frontal sections are shown for all histological evaluations. MB morphology is shown in animals expressing pan-neuronally the p*UAS–htau*$^{2N4R–FLAG}$ transgene (WT) or the p*UAS–htau*$^{2N4R–STA–FLAG}$ variant (STA) at the levels of the calyces (1, 2), pedunculus and ellipsoid body (3, 4), α/β lobes (5, 6), and the γ lobes (7, 8). The deficits in MB morphology in animals accumulating 2N4R–FLAG hTau were not apparent during accumulation of the 2N4R–STA–FLAG protein. ***B***, A representative Western blot of head lysates from animals expressing the indicated Tau proteins pan-neuronally probed with the T46 anti-Tau antibody. Syntaxin (Syx) was used as loading control. Quantification of the protein levels relative to that of WT (black bar arbitrarily set to 1) from three independent such blots. Statistical analysis did not reveal significant differences in the levels of these proteins. ***C***, Associative olfactory learning performance of animals accumulating Tau pan-neuronally that lack MB structural aberrations (gray bars) and their matching genetic controls of transgene insertion heterozygotes without the *Elav*–Gal4 driver (respective black bars) and driver heterozygotes alone (white bars). $n \geq 8$ for all genotypes. ANOVA indicated significant differences in performance ($F_{(6,68)} = 192.1491$, $p < 0.0001$) and subsequent contrast analysis between control, and experimental strains as indicated by the lines revealed highly significant differences (*$p < 0.0001$) in the performance of *bTau* and $htau^{2N4R–STA–FLAG}$-expressing animals from their non-expressing respective controls but not between animals expressing $htau^{R406W-S2A}$ and their controls. ***D***, Olfactory acuity of Tau-expressing animals relative to the *Elav*/+ controls measured as avoidance of the 3-octanol (OCT) and benzaldehyde (BNZ) odors used in conditioning. ANOVA for 3-octanol avoidance indicated significant differences ($F_{(3,32)} = 5.4252$, $p < 0.05$). Subsequent Tukey's honestly significant difference analysis at $\alpha = 0.05$ indicated that relative to controls only the performance of bTau-accumulating animals was significantly different (asterisk). In contrast, ANOVA for benzaldehyde avoidance did not indicate significant differences in performance ($F_{(3,30)} = 2.6299$, $p < 0.096$).

Although structurally intact, the MBs of $htau^{2N4R–STA}$-expressing flies could be dysfunctional as they are during bTau

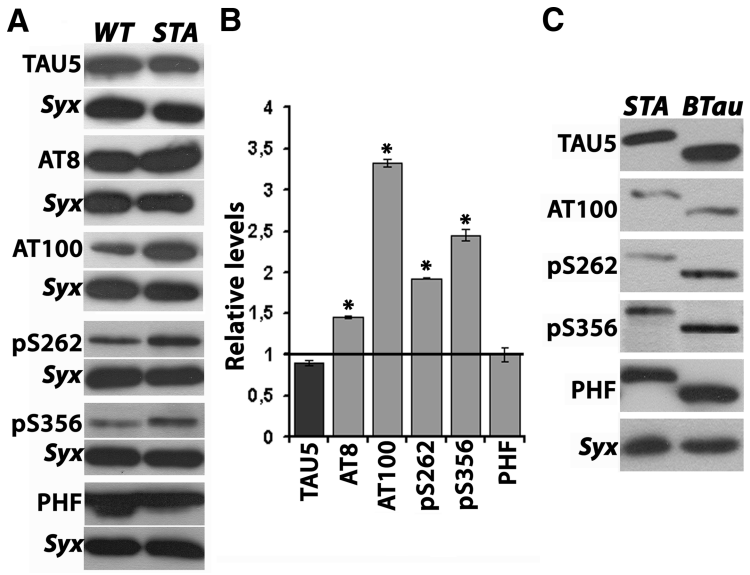

Figure 7. Enhanced phosphorylation at specific disease-specific sites in 2N4RSTA-accumulating animals. ***A***, Representative Western blots from head lysates of flies accumulating 2N4R–FLAG (WT) and 2N4R–STA–FLAG (STA) probed with the antibodies indicated on the right. The level of syntaxin (Syx) in the lysates was used as control for quantifications. The TAU5 antibody measures total Tau in the lysates, whereas all others target particular phosphorylated residues. ***B***, Quantification of at least three independent blots and extracts as those shown in ***A***. The syntaxin-normalized level of 2N4R–FLAG for each quantification was fixed to 1 and represented by the horizontal line. The bars then represent the mean ± SEM relative levels of 2N4R–STA–FLAG phosphorylated at the given sites, over that of the 2N4R–FLAG control. ANOVA indicated significant differences ($F_{(5,18)} = 358.527, p < 0.0001$) and subsequent Tukey's honestly significant difference test at $\alpha = 0.05$ demonstrated that means marked by asterisks were significantly different from controls, except for those for the anti-TAU5 (total) and anti-PHF. ***C***, Representative Western blots from head lysates of animals accumulating bTau pan-neuronally compared with similar lysates from 2N4R–STA-accumulating animals, probed with the antibodies detecting enhanced occupation of particular sites in the latter protein.

accumulation (Mershin et al., 2004). Because the MBs are essential for learning and memory (Heisenberg, 2003; Davis, 2005), disruption of these processes constitutes a sensitive measure of their functional integrity (Skoulakis and Grammenoudi, 2006). Therefore, we subjected these animals to an olfactory associative learning task (Mershin et al., 2004). Performance in this task was severely impaired for animals accumulating bTau compared with *Elav* and *btau*/+ heterozygous controls (Fig. 6*C*). Heterozygotes did not exhibit behavioral deficits, demonstrating that transgene insertions are not causal of the phenotype. Significantly, accumulation of 2N4R^{STA} at equal levels with bTau also precipitated highly deficient learning compared with *STA*/+ animals, albeit not to the degree exhibited by flies expressing *btau*. A similar deficit was exhibited by an independent UAS–*2N4R*^{STA} line (supplemental Fig. 5*B*, available at www.jneurosci.org as supplemental material). We did not test animals expressing *htau*$^{2N4R–FLAG}$ because their structurally aberrant MBs were not expected to support associative learning (de Belle and Heisenberg, 1994), as shown for animals expressing other WT *htau* transgenes (Grammenoudi et al., 2008). Flies expressing *htau*^{R406W}, which harbor defective MBs, were also reported defective in this task (Grammenoudi et al., 2008). These learning deficits, however, are not precipitated simply by the presence of the human protein in the fly CNS, because animals accumulating the benign R406WS2A variant performed equally well with controls (Fig. 6*C*). These results demonstrate that, despite their apparent structural integrity, the presence of approximately equal levels of bTau and 2N4R^{STA} but not R406WS2A resulted in MB dysfunction.

Animals expressing *btau* and all other experimental strains exhibited normal avoidance of the electric footshock unconditioned stimulus (supplemental Fig. 5*C*, available at www.jneurosci.org as supplemental material), a necessary precondition for normal learning in this paradigm (Tully and Quinn, 1985). In contrast, *btau*-expressing animals exhibited significantly lower avoidance of octanol and somewhat elevated avoidance of benzaldehyde. Octanol avoidance of flies accumulating 2N4R^{STA} was somewhat lower but was not significantly different from controls, and responses to benzaldehyde were normal (Fig. 6*D*). It is unclear whether and how enhanced benzaldehyde avoidance may affect associative learning in this paradigm. Nevertheless, the results suggest that at least part of the strong learning deficit of *btau*-expressing animals is the result of impaired or altered olfactory responses. Because bTau accumulates pan-neuronally and given that its accumulation specifically within MBs results in their dysfunction (herein and Mershin et al., 2004), it is not surprising that it may also result in dysfunction of the olfactory system or higher-order neurons mediating direct response to odors (Tanaka et al., 2004). The functional consequences of 2N4R^{STA} in the olfactory system were marginal if at all. The greater dysfunction precipitated by bTau may also be the result of the additional differences between the two proteins, especially in their N-terminal halves including the extensions, as illustrated in supplemental Figure 5*A* (available at www.jneurosci.org as supplemental material). Nevertheless, it appears that replacing Ser^{238} and Thr^{245} with nonphosphorylatable residues rendered the effects of 2N4R–hTau more like those of bTau, yielding intact but dysfunctional MBs.

To investigate potential effects of mutating Ser^{238} and Thr^{245} on Tau phosphorylation, we tested 2N4R^{STA} for occupation of key sites typically involved in pathology and possibly pathogenesis in humans (Augustinack et al., 2002; Geschwind, 2003; Stoothoff and Johnson, 2005) and *Drosophila* (Nishimura et al., 2004; Steinhilb et al., 2007a,b). Given the lack of MB morphological deficits during *htau*$^{2N4R–STA}$ expression and the association of hyperphosphorylation with toxicity and pathology, we hypothesized that 2N4R^{STA} may be underphosphorylated relative to 2N4R. Multiple independent quantitative Western blots represented in Figure 7*A* were quantified in Figure 7*B*. We used a different antibody (TAU5) targeting the PRD rather than the C-terminus-targeted T46 used previously (Fig. 6*B*) to assess independently the levels of the two proteins. The steady-state level of 2N4R^{STA} was not significantly different from that of the 2N4R control (Fig. 7*B*). The blots also demonstrate that, as expected (Grammenoudi et al., 2006), the 2N4R protein was phosphorylated at epitopes at the AT8, AT100, pS262, pS356, and PHF (Fig. 7*A*). Surprisingly, however, phosphorylation of 2N4R^{STA} appeared significantly elevated over that of 2N4R at the AT8, AT100, pS262, and pS356 sites, whereas no change was detectable at the PHF epitope. Thus, in contrast to our hypothesis, the S238A and T245A mutations resulted in hyperphosphorylation at the sites defined by the AT8, pS262, and pS356 antigenic sites but also increased abnormal phosphorylation as detected by the

Table 2. Summary table of MB structural and functional defects during pan-neuronal Tau accumulation

Transgenic protein	Disease association	MB integrity	MB function (learning)	Origin
dTau	N	Normal	Defective	Mershin et al., 2004
bTau	N	Normal	Defective	Ito et al., 1997b
0N3R	AD	Normal	Normal	Mudher et al., 2004
0N4R	AD	Ablation	Defective	Wittmann et al., 2001
2N4R	AD	Ablation	Defective	Gift from J. Botas
$0N4R^{R406W}$	FTDP-17	Defective	Defective	Wittmann et al., 2001
$0N4R^{V377M}$	FTDP-17	Mild defect	Mild defect	Wittmann et al., 2001
$0N4R^{E14}$	N	Ablation		Steinhilb et al., 2007
$0N4R^{AP}$	N	Normal		Steinhilb et al., 2007
$0N4R^{R406WS2A}$	N	Normal	Normal	Nishimura et al., 2004
$2N4R^{S2A}$	N	Normal		Chatterjee et al., 2009
2N4R—Flag	AD	Defective		This study
$2N4R^{STA}$—Flag	N	Normal	Defective	This study

The transgenes used in this and previous studies (Grammenoudi et al., 2008) are indicated in the first column. Association of each transgenic Tau isoform is listed in the second column. N, Non-association. Origin refers to the source of the transgenes used.

AT100 antibody, which is typically associated with AD pathology in humans (Matsuo et al., 1994; Mailliot et al., 1998; Buée et al., 2000; Sergeant et al., 2005). Of the hTau isoforms that do not precipitate MB structural defects, only R406WS2A was inefficiently phosphorylated at AT100, in addition to the lack of phosphates at the mutated Ser^{262} and Ser^{356} (Nishimura et al., 2004; Grammenoudi et al., 2006).

Interestingly, AT100 and Ser^{356} are the sites that exhibited the highest phosphorylation on $2N4R^{STA}$. Given the lack of learning deficits in R406WS2A and the strong impairment of $htau^{2N4R–STA}$-expressing animals, it is possible that hyperphosphorylation at these sites may result in dysfunction rather than toxicity in MB neurons. Consistent with this notion, bTau, which contains alanines at positions 238 and 245, is also phosphorylated at the epitopes with enhanced occupancy on $2N4R^{STA}$. Notably, the AT100 epitope is also occupied in bTau, strengthening the interpretation that this abnormal phosphorylation in the MBs is correlated with dysfunction rather than toxicity because neurons accumulating it appear intact. These results then are congruent with the notion that the mutations at Ser^{238} and Thr^{245} render the 2N4R hTau functionally similar to bTau (Fig. 7*C*). Therefore, these mutations dissociate hTau toxicity on MB neuroblasts and dysfunction of adult MBs. Although in progress, we currently lack the antibodies to unequivocally demonstrate occupation of Ser^{238} and Thr^{245} in the *Drosophila* CNS. Nevertheless, our data suggest that Ser^{238} and Thr^{245} phosphorylations are required, probably in addition to hyperphosphorylation at the known sites mentioned above, in the genesis of MB morphological defects. Hence, we have defined two novel sites on hTau likely implicated in the pathogenesis of tauopathies.

Discussion

A novel hTau-dependent deficit in the CNS

Excess hTau results in age-dependent degeneration and vacuolization in the *Drosophila* CNS (for review, see Khurana, 2008). Here we describe a novel type of hTau-dependent toxicity that occurs within a narrow temporal window early in embryogenesis and specifically targets MBNBs. Collective data from this and previous studies (Grammenoudi et al., 2008) on the effects of WT and mutant Tau accumulation on MB structure and function are presented in Table 2. MB defects may have been unnoticed in previous studies (Wittmann et al., 2001; Ghosh and Feany, 2004; Khurana et al., 2006) for the following reasons. First, we focused specifically on structural analysis of the MBs because pan-neuronal accumulation of hTau isoforms resulted in olfactory learning deficits (Grammenoudi et al., 2008), and these neurons are essential for these processes (Heisenberg, 2003). Previous analyses of the effects of pan-neuronal accumulation of hTau (Wittmann et al., 2001; Ghosh and Feany, 2004; Khurana et al., 2006) focused in the central brain perhaps for ease and consistency in scoring vacuolization. However, we show that the ellipsoid body and remaining central brain neuropils were not affected by hTau in young flies. Second, we used the anti-LEO antibody (Skoulakis and Davis, 1996) for our analysis, which, unlike mass histology methods, affords enhanced resolution of these neurons. Finally, based on previous observations (Grammenoudi et al., 2008), we initially focused on the effects of WT hTaus. In contrast, studies that concentrated on CNS vacuolization used mostly the R406W mutant (Wittmann et al., 2001; Dias-Santagata et al., 2007; Fulga et al., 2007), which precipitates milder MB phenotypes in a smaller proportion of animals (Table 1).

Similar to Tau toxicity on MB development, retina defects also occur during the brief period that ommatidial precursor cells spend in the morphogenetic furrow undergoing the final round of mitoses and commitment to their cellular fates (Thomas and Wassarman, 1999). However, there are distinct differences in Tau toxicity in retina and MBs. The R406W and V377M mutant isoforms, which typically exhibit the strongest vacuolization in the aged CNS (Wittmann et al., 2001; Dias-Santagata et al., 2007; Fulga et al., 2007) and retina disruption (Jackson et al., 2002; Nishimura et al., 2004; Khurana et al., 2006; Steinhilb et al., 2007b), yielded milder and less penetrant MB phenotypes (Table 1). It appears therefore that WT hTau isoforms and especially the longer 2N4R Tau typically associated with AD yield more severe penetrant effects on MB integrity in contrast to the milder defects precipitated by the FTDP-17-linked mutant alleles. Unlike 0N3R, which bound less efficiently to microtubules in adult brain extracts, such differences were not uncovered among the other WT and mutant Taus (data not shown). Therefore, differential microtubule binding does not explain differences in the effects on MB development.

Our data (Fig. 4) (supplemental Figs. 2, 3, available at www.jneurosci.org as supplemental material) suggest that accumulation of particular hTau isoforms in MBNBs does not seem to lead to apoptosis or an obvious change of developmental fate. Hence, we propose in future experiments to address the hypothesis that defects may arise because of Tau-dependent suppression of

MBNB proliferation. We suggest that hTau accumulation in MBNBs or their precursors may disrupt protein complexes and processes requisite for asymmetric cell division, which permits MBNBs to continue generating GMCs and eventually the 2500 neurons of each MB. Premature normal cell cycle activation in the MBNBs and the consequent symmetrical divisions may then result in loss of their stem cell properties (Doe, 2008), resulting in fewer GMCs and rarefaction of their descendant MB neurons. This notion is consistent with reports that hTau in the adult retina and the brain activates the cell cycle ectopically, resulting in apoptosis, a potential explanation of vacuolization (Khurana et al., 2006) in brain areas different from the MBs.

It is intriguing that blocking putative phosphorylation of the potential atypical PKC targets Ser^{238} and Thr^{245} suppressed hTau MB toxicity. Atypical PKC is involved in establishing cell polarity, essential for the asymmetric divisions required to regulate self-renewal as opposed to differentiation (Doe, 2008). Thus, we propose that, in MBNBs, hTau may sequester atypical PKC away from complexes requisite to maintain polarity and their self-renewal, or it interferes directly with the process. Interestingly, recent reports suggest that excess Tau may differentially target neural stem cells in the dentate gyrus and the subventricular zone responsible for adult neurogenesis in the mouse and human patients (for review, see Thompson et al., 2008). Therefore, hTau toxicity on MBNBs may represent an analogous phenomenon in the fly but manifested in the embryo because of their unique developmental properties (Ito et al., 1997a).

On a practical note, $hTau^{0N4R–E14}$ and $hTau^{2N4R}$, which consistently yielded type 2 defects in the majority of animals, could be used experimentally as a nonchemical method of MB ablation (de Belle and Heisenberg, 1994), yielding earlier and possibly more extensive deficits.

Phosphorylation on specific sites mediates Tau-dependent toxicity and dysfunction of the MBs

Hyperphosphorylation of Tau, especially at particular sites, often used as diagnostic in human tauopathies is requisite for pathogenesis (Avila et al., 2004; Sergeant et al., 2008). Similarly, MBNB toxicity appears to require Tau hyperphosphorylation because it is enhanced by the highly pathogenic phosphomimic $0N4R^{E14}$ protein and suppressed by the underphosphorylated $0N4R^{AP}$ (Fig. 5). Our data suggest that phosphorylation at specific sites, rather than hyperphosphorylation per se, appears differentially implicated in Tau-mediated MB toxicity and dysfunction.

MBNB toxicity appears to require phosphorylation at Ser^{262} and Ser^{356}, possibly by Par-1 as suggested (Nishimura et al., 2004; Chatterjee et al., 2009), because blocking it in the context of the R406W mutation (Fig. 5*B*) (supplemental Fig. 4*B*, available at www.jneurosci.org as supplemental material) or WT 2N4R (supplemental Fig. 4*D*, available at www.jneurosci.org as supplemental material) yielded normal MBs. Retina toxicity was also eliminated by blocking phosphorylation of these sites (Nishimura et al., 2004; Chatterjee et al., 2009). These data suggest that, as in the retina, Par-1-targeted sites may also act as facilitators of additional phosphorylation in the MBNBs. Enhanced phosphorylation after Ser^{262} and Ser^{356} occupation is prominent at the GSK3β-targeted (Plattner et al., 2006), AD-relevant epitopes AT8, AT100, and PHF-1 among others (Nishimura et al., 2004; Chatterjee et al., 2009). Interestingly, unlike in the R406W mutant (Nishimura et al., 2004), blocking Par-1 phosphorylation eliminated 2N4R toxicity in the retina, but phosphorylation remained elevated at the latter epitopes (Chatterjee et al., 2009). This suggests that occupation of these sites may occur via distinct mechanisms in the context of mutant and WT Tau isoforms and perhaps even have distinct functional consequences.

Furthermore, we demonstrate that hTau-dependent MBNB toxicity appears to require novel phosphorylations at Ser^{238} and Thr^{245}, because blocking them by substituting alanines eliminated MB aberrations. Congruently, the equivalent sites in bTau, which is not toxic on the MBNBs, lack phosphorylatable residues, further underscoring the importance of these phosphorylations for pathology. However, these sites appear implicated in Tau-mediated dysfunction because, although the MBs are intact in flies accumulating $2N4R^{STA}$, they are unable to support normal associative learning (Fig. 6*B*). Surprisingly, phosphorylation at epitopes typically associated with toxicity and neurodegeneration, such as AT8, AT100, and the Par-1 targets Ser^{262} and Ser^{356}, was elevated in these animals (Fig. 7*A*). Therefore, it appears that putative phosphorylation on Ser^{238} and Thr^{245} normally suppresses, at least in part, phosphorylation at these epitopes, and therefore their blockade by alanines yields the observed enhanced phosphorylation on $2N4R^{STA}$. Nevertheless, hyperphosphorylation at these sites, although necessary (Nishimura et al., 2004; Chatterjee et al., 2009), was not sufficient for MBNB toxicity without the putative Ser^{238} and Thr^{245} occupation. Therefore, we have identified two novel putatively phosphorylated residues apparently essential for the toxicity and neurodegeneration associated with excess Tau accumulation in *Drosophila* and possibly in human patients as well.

We also dissociated Tau toxicity from dysfunction in *Drosophila* by blocking Ser^{238} and Thr^{245} phosphorylation. These sites may also be involved in pathology or behavioral deficits associated with human tauopathies as suggested (Sergeant et al., 2008), but this assignment requires verification.

Interestingly, these results suggest that hyperphosphorylation of AT8, AT100, pS262, and pS356 does not always precipitate toxicity and neurodegeneration. Rather, their effects may depend on positive and negative contribution of additional Tau phosphorylations, possibly the temporal order of phosphorylations and the neuronal type in which they occur. In the absence of Ser^{238} and Thr^{245} phosphorylation, enhanced occupation of these sites leads to dysfunctional MBs. In the context of the intact adult MB neurons of $2N4R^{STA}$-accumulating flies, our data suggest that augmented phosphorylation at Ser^{262}/Ser^{356} and the consequent AT100 occupation by analogy to the retina (Nishimura et al., 2004) are involved in the Tau-mediated learning deficits. This is supported by the lack of learning deficits by animals accumulating R406WS2A protein (Fig. 6*C*), in which blockade of Ser^{262} and Ser^{356} phosphorylation results in suppressed phosphorylation at AT100 (Grammenoudi et al., 2006). Thus, these sites, whose phosphorylation has been linked to toxicity in the fly retina and are thought of clinical relevance in human AD patients, may have distinct roles in dysfunction and degeneration in the context of additional Tau phosphorylation at particular sites and the cellular context in which these occur. It is possible that, in fly and human neurons accumulating Tau, phosphorylation at Ser^{238}/Thr^{245} may follow occupation of Ser^{262}/Ser^{356} and AT100, perhaps reflecting the transition from dysfunctional to degenerating neurons, or they may occur independently. Investigating these possibilities may lead to better understanding of dysfunction and degeneration and the possible transition between them that characterize tauopathies.

References

Acevedo SF, Froudarakis EI, Tsiorva AA, Skoulakis EM (2007) Distinct neuronal circuits mediate experience-dependent, non-associative osmotactic responses in *Drosophila*. Mol Cell Neurosci 34:378–389.

Alonso Adel C, Mederlyova A, Novak M, Grundke-Iqbal I, Iqbal K (2004) Promotion of hyperphosphorylation by frontotemporal dementia tau mutations. J Biol Chem 279:34873–34881.

Amano M, Kaneko T, Maeda A, Nakayama M, Ito M, Yamauchi T, Goto H, Fukata Y, Oshiro N, Shinohara A, Iwamatsu A, Kaibuchi K (2003) Identification of Tau and MAP2 as novel substrates of Rho-kinase and myosin phosphatase. J Neurochem 87:780–790.

Augustinack JC, Schneider A, Mandelkow EM, Hyman BT (2002) Specific tau phosphorylation sites correlate with severity of neuronal cytopathology in Alzheimer's disease. Acta Neuropathol 103:26–35.

Avila J, Lucas JJ, Perez M, Hernandez F (2004) Role of tau protein in both physiological and pathological conditions. Physiol Rev 84:361–384.

Berger C, Renner S, Lüer K, Technau GM (2007) The commonly used marker ELAV is transiently expressed in neuroblasts and glial cells in the *Drosophila* embryonic CNS. Dev Dyn 236:3562–3568.

Brand AH, Perrimon N (1993) Targeted gene expression as a means of altering cell fates and generating dominant phenotypes. Development 118:401–415.

Buée L, Bussière T, Buée-Scherrer V, Delacourte A, Hof PR (2000) Tau protein isoforms, phosphorylation and role in neurodegenerative disorders. Brain Res Brain Res Rev 33:95–130.

Chatterjee S, Sang TK, Lawless GM, Jackson GR (2009) Dissociation of tau toxicity and phosphorylation: role of GSK-3beta, MARK and Cdk5 in a *Drosophila* model. Hum Mol Genet 18:164–177.

Chee FC, Mudher A, Cuttle MF, Newman TA, MacKay D, Lovestone S, Shepherd D (2005) Overexpression of tau results in defective synaptic transmission in *Drosophila* neuromuscular junctions. Neurobiol Dis 20:918–928.

Clark ME, Anderson CL, Cande J, Karr TL (2005) Widespread prevalence of Wolachia in laboratory stocks and the implications for *Drosophila* research. Genetics 170:1667–1675.

Crittenden JR, Skoulakis EM, Han KA, Kalderon D, Davis RL (1998) Tripartite mushroom body architecture revealed by antigenic markers. Learn Mem 5:38–51.

Davis RL (2005) Olfactory memory formation in *Drosophila*: from molecular to systems neuroscience. Annu Rev Neurosci 28:275–302.

de Belle JS, Heisenberg M (1994) Associative odor learning in *Drosophila* abolished by chemical ablation of mushroom bodies. Science 263:692–695.

Delacourte A (2005) Tauopathies: recent insights into old diseases. Folia Neuropathologica 43:244–257.

DeTure M, Ko LW, Yen S, Nacharaju P, Easson C, Lewis J, van Slegtenhorst M, Hutton M, Yen SH (2000) Missense tau mutations identified in FTDP-17 have a small effect on tau-microtubule interactions. Brain Res 853:5–14.

Dias-Santagata D, Fulga TA, Duttaroy A, Feany MB (2007) Oxidative stress mediates tau-induced neurodegeneration in *Drosophila*. J Clin Invest 117:236–245.

Doe CQ (2008) Neural stem cells: balancing self-renewal with differentiation. Development 135:1575–1587.

Fulga TA, Elson-Schwab I, Khurana V, Steinhilb ML, Spires TL, Hyman BT, Feany MB (2007) Abnormal bundling and accumulation of F-actin mediates tau-induced neuronal degeneration in vivo. Nat Cell Biol 9:139–148.

Geschwind DH (2003) Tau phosphorylation, tangles, and neurodegeneration: the chicken or the egg? Neuron 40:457–460.

Ghosh S, Feany MB (2004) Comparison of pathways controlling toxicity in the eye and brain in *Drosophila* models of human neurodegenerative diseases. Hum Mol Genet 13:2011–2018.

Goedert M (2005) Tau gene mutations and their effects. Mov Disord 20 [Suppl 12]:S45–S52.

Grammenoudi S, Kosmidis S, Skoulakis EM (2006) Cell type-specific processing of human Tau proteins in *Drosophila*. FEBS Lett 580:4602–4606.

Grammenoudi S, Anezaki M, Kosmidis S, Skoulakis EMC (2008) Modeling cell and isoform type specificity of tauopathies in *Drosophila*. In: Symposia of the Society for Experimental Biology (Mudher A, Chapman T, eds), pp 39–56. London: Taylor and Francis.

Hartenstein V, Younossi-Hartenstein A, Lekven A (1994) Delamination and division in the *Drosophila* neuroectoderm: spatio-temporal pattern, cytoskeletal dynamics, and common control by neurogenic and segment polarity genes. Dev Biol 165:480–499.

Heisenberg M (2003) Mushroom body memoir: from maps to models. Nat Rev Neurosci 4:266–275.

Ishihara T, Zhang B, Higuchi M, Yoshiyama Y, Trojanowski JQ, Lee VM (2001) Age-dependent induction of congophilic neurofibrillary tau inclusions in tau transgenic mice. Am J Pathol 158:555–562.

Ito K, Hotta Y (1992) Proliferation pattern of postembryonic neuroblasts in the brain of *Drosophila melanogaster*. Dev Biol 149:134–148.

Ito K, Awano W, Suzuki K, Hiromi Y, Yamamoto D (1997a) The *Drosophila* mushroom body is a quadruple structure of clonal units each of which contains a virtually identical set of neurones and glial cells. Development 124:761–771.

Ito K, Sass H, Urban J, Hofbauer A, Schneuwly S (1997b) GAL4-responsive UAS-tau as a tool for studying the anatomy and development of the *Drosophila* central nervous system. Cell Tissue Res 290:1–10.

Jackson GR, Wiedau-Pazos M, Sang TK, Wagle N, Brown CA, Massachi S, Geschwind DH (2002) Human wild-type tau interacts with wingless pathway components and produces neurofibrillary pathology in *Drosophila*. Neuron 34:509–519.

Khurana V (2008) Modeling tauopathy in the fruit fly *Drosophila melanogaster*. J Alzheimers Dis 15:541–553.

Khurana V, Lu Y, Steinhilb ML, Oldham S, Shulman JM, Feany MB (2006) TOR-mediated cell-cycle activation causes neurodegeneration in a *Drosophila* tauopathy model. Curr Biol 16:230–241.

Kimura T, Yamashita S, Fukuda T, Park JM, Murayama M, Mizoroki T, Yoshiike Y, Sahara N, Takashima A (2007) Hyperphosphorylated tau in parahippocampal cortex impairs place learning in aged mice expressing wild-type human tau. EMBO J 26:5143–5152.

Lee VM, Kenyon TK, Trojanowski JQ (2005) Transgenic animal models of tauopathies. Biochim Biophys Acta 1739:251–259.

Lee VM, Goedert M, Trojanowski JQ (2001) Neurodegenerative tauopathies. Annu Rev Neurosci 24:1121–1159.

Leyssen M, Ayaz D, Hébert SS, Reeve S, De Strooper B, Hassan BA (2005) Amyloid precursor protein promotes post-developmental neurite arborization in the *Drosophila* brain. EMBO J 24:2944–2955.

Lin DM, Goodman CS (1994) Ectopic and increased expression of Fasciclin II alters motoneuron growth cone guidance. Neuron 13:507–523.

Mailliot C, Bussière T, Caillet-Boudin ML, Delacourte A, Buée L (1998) Alzheimer-specific epitope of AT100 in transfected cell lines with tau: toward an efficient cell model of tau abnormal phosphorylation. Neurosci Lett 255:13–16.

Martini SR, Davis RL (2005) The dachshund gene is required for the proper guidance and branching of mushroom body axons in *Drosophila melanogaster*. J Neurobiol 64:133–144.

Martini SR, Roman G, Meuser S, Mardon G, Davis RL (2000) The retinal determination gene, dachshund, is required for mushroom body cell differentiation. Development 127:2663–2672.

Matsuo ES, Shin RW, Billingsley ML, Van deVoorde A, O'Connor M, Trojanowski JQ, Lee VM (1994) Biopsy-derived adult human brain tau is phosphorylated at many of the same sites as Alzheimer's disease paired helical filament tau. Neuron 13:989–1002.

McGuire SE, Le PT, Osborn AJ, Matsumoto K, Davis RL (2003) Spatiotemporal rescue of memory dysfunction in *Drosophila*. Science 302:1765–1768.

McGuire SE, Mao Z, Davis RL (2004) Spatiotemporal gene expression targeting with the TARGET and gene-switch systems in *Drosophila*. Sci STKE 2004:pl6.

Menzel R (2001) Searching for the memory trace in a mini-brain, the honeybee. Learn Mem 8:53–62.

Mershin A, Pavlopoulos E, Fitch O, Braden BC, Nanopoulos DV, Skoulakis EM (2004) Learning and memory deficits upon TAU accumulation in *Drosophila* mushroom body neurons. Learn Mem 11:277–287.

Moressis A, Friedrich AR, Pavlopoulos E, Davis RL, Skoulakis EMC (2009) A dual role for the adaptor protein DRK in *Drosophila* olfactory learning and memory. J Neurosci 29:2611–2625.

Mudher A, Shepherd D, Newman TA, Mildren P, Jukes JP, Squire A, Mears A, Drummond JA, Berg S, MacKay D, Asuni AA, Bhat R, Lovestone S (2004) GSK-3beta inhibition reverses axonal transport defects and behavioural phenotypes in *Drosophila*. Mol Psychiatry 9:522–530.

Nishimura I, Yang Y, Lu B (2004) PAR-1 kinase plays an initiator role in a

temporally ordered phosphorylation process that confers tau toxicity in *Drosophila*. Cell 116:671–682.

Noveen A, Daniel A, Hartenstein V (2000) Early development of the *Drosophila* mushroom body: the roles of *eyless* and *dachshund*. Development 127:3475–3488.

Patel NH (1994) Imaging neuronal subsets and other cell types in whole-mount *Drosophila* embryos and larvae using antibody probes. Methods Cell Biol 44:445–487.

Philip N, Acevedo SF, Skoulakis EM (2001) Conditional rescue of olfactory learning and memory defects in mutants of the 14-3-3ζ gene leonardo. J Neurosci 21:8417–8425.

Plattner F, Angelo M, Giese KP (2006) The roles of cyclin-dependent kinase 5 and glycogen synthase kinase 3 in tau hyperphosphorylation. J Biol Chem 281:25457–25465.

Raabe T, Clemens-Richter S, Twardzik T, Ebert A, Gramlich G, Heisenberg M (2004) Identification of mushroom body miniature, a zinc-finger protein implicated in brain development of *Drosophila*. Proc Natl Acad Sci U S A 101:14276–14281.

Reed LA, Wszolek ZK, Hutton M (2001) Phenotypic correlations in FTDP-17. Neurobiol Aging 22:89–107.

Robinow S, White K (1988) The locus elav of *Drosophila melanogaster* is expressed in neurons at all developmental stages. Dev Biol 126:294–303.

Robinow S, White K (1991) Characterization and spatial distribution of the ELAV protein during *Drosophila melanogaster* development. J Neurobiol 22:443–461.

Sang TK, Jackson GR (2005) *Drosophila* models of neurodegenerative disease. NeuroRx 2:438–446.

Santacruz K, Lewis J, Spires T, Paulson J, Kotilinek L, Ingelsson M, Guimaraes A, DeTure M, Ramsden M, McGowan E, Forster C, Yue M, Orne J, Janus C, Mariash A, Kuskowski M, Hyman B, Hutton M, Ashe KH (2005) Tau suppression in a neurodegenerative mouse model improves memory function. Science 309:476–481.

Schindowski K, Bretteville A, Leroy K, Bégard S, Brion JP, Hamdane M, Buée L (2006) Alzheimer's disease-like tau neuropathology leads to memory deficits and loss of functional synapses in a novel mutated tau transgenic mouse without any motor deficits. Am J Pathol 169:599–616.

Sergeant N, Delacourte A, Buée L (2005) Tau protein as a differential biomarker of tauopathies. Biochim Biophys Acta 1739:179–197.

Sergeant N, Bretteville A, Hamdane M, Caillet-Boudin ML, Grognet P, Bombois S, Blum D, Delacourte A, Pasquier F, Vanmechelen E, Schraen-Maschke S, Buée L (2008) Biochemistry of Tau in Alzheimer's disease and related neurological disorders. Expert Rev Proteomics 5:207–224.

Shiarli AM, Jennings R, Shi J, Bailey K, Davidson Y, Tian J, Bigio EH, Ghetti B, Murrell JR, Delisle MB, Mirra S, Crain B, Zolo P, Arima K, Iseki E, Murayama S, Kretzschmar H, Neumann M, Lippa C, Halliday G, et al. (2006) Comparison of extent of tau pathology in patients with frontotemporal dementia with Parkinsonism linked to chromosome 17 (FTDP-17), frontotemporal lobar degeneration with Pick bodies and early onset Alzheimer's disease. Neuropathol Appl Neurobiol 32:374–387.

Skoulakis EM, Davis RL (1996) Olfactory learning deficits in mutants for leonardo, a *Drosophila* gene encoding a 14-3-3 protein. Neuron 17:931–944.

Skoulakis EM, Grammenoudi S (2006) Dunces and da Vincis: the genetics of learning and memory in *Drosophila*. Cell Mol Life Sci 63:975–988.

Steinhilb ML, Dias-Santagata D, Fulga TA, Felch DL, Feany MB (2007a) Tau phosphorylation sites work in concert to promote neurotoxicity in vivo. Mol Biol Cell 18:5060–5068.

Steinhilb ML, Dias-Santagata D, Mulkearns EE, Shulman JM, Biernat J, Mandelkow EM, Feany MB (2007b) S/P and T/P phosphorylation is critical for tau neurotoxicity in *Drosophila*. J Neurosci Res 85:1271–1278.

Stoothoff WH, Johnson GV (2005) Tau phosphorylation: physiological and pathological consequences. Biochim Biophys Acta 1739:280–297.

Strausfeld NJ (1976) Atlas of an insect brain. New York: Springer.

Strausfeld NJ, Sinakevitch I, Vilinsky I (2003) The mushroom bodies of *Drosophila melanogaster*: an immunocytological and golgi study of Kenyon cell organization in the calyces and lobes. Microsc Res Tech 62:151–169.

Struhl G, Fitzgerald K, Greenwald I (1993) Intrinsic activity of the Lin-12 and Notch intracellualr domains in vivo. Cell 74:331–345.

Tanaka NK, Awasaki T, Shimada T, Ito K (2004) Integration of chemosensory pathways in the *Drosophila* second-order olfactory centers. Curr Biol 14:449–457.

Tettamanti M, Armstrong JD, Endo K, Yang MY, Furukubo-Tokunaga K, Kaiser K, Reichert H (1997) Early development of the *Drosophila* mushroom bodies, brain centres for associative learning and memory. Dev Genes Evol 207:242–252.

Thomas BJ, Wassarman DA (1999) A fly's eye view of biology. Trends Genet 15:184–190.

Thompson A, Boekhoorn K, Van Dam AM, Lucassen PJ (2008) Changes in adult neurogenesis in neurodegenerative diseases: cause or consequence? Genes Brain Behav 7 [Suppl 1]:28–42.

Trojanowski JQ, Lee VM (2005) Pathological tau: a loss of normal function or a gain in toxicity? Nat Neurosci 8:1136–1137.

Tully T, Quinn WG (1985) Classical conditioning and retention in normal and mutant *Drosophila melanogaster*. J Comp Physiol A 157:263–277.

Tzortzopoulos A, Skoulakis EMC (2007) Paternally and maternally transmitted GAL4 transcripts contribute to UAS transgene expression in early *Drosophila* embryos. Genesis 45:737–743.

Wittmann CW, Wszolek MF, Shulman JM, Salvaterra PM, Lewis J, Hutton M, Feany MB (2001) Tauopathy in *Drosophila*: neurodegeneration without neurofibrillary tangles. Science 293:711–714.

Yeh E, Gustafson K, Boulianne GL (1995) Green fluorescent protein as a vital marker and reporter of gene expression in *Drosophila*. Proc Natl Acad Sci U S A 92:7036–7040.

Younossi-Hartenstein A, Nassif C, Green P, Hartenstein V (1996) Early neurogenesis of the *Drosophila* brain. J Comp Neurol 370:313–329.

Zhou L, Schnitzler A, Agapite J, Schwartz LM, Steller H, Nambu JR (1997) Cooperative functions of the reaper and head involution defective genes in the programmed cell death of *Drosophila* central nervous system midline cells. Proc Natl Acad Sci U S A 94:5131–5136.

Zhu S, Lin S, Kao CF, Awasaki T, Chiang AS, Lee T (2006) Gradients of the *Drosophila* Chinmo BTB-zinc finger protein govern neuronal temporal identity. Cell 127:409–422.